An analysis of the thickness vibration of an unelectroded doubly-rotated quartz circular plate

Longtao Xie,[1] Shaoyun Wang,[1] Chuanzeng Zhang,[2] and Ji Wang[1,a)]
[1]*Piezoelectric Device Lab, School of Mechanical Engineering & Mechanics, Ningbo University, Ningbo, 315211, China*
[2]*Department of Civil Engineering, University of Siegen, Siegen, D-57068, Germany*

(Received 28 May 2018; revised 31 July 2018; accepted 31 July 2018; published online 17 August 2018)

The scalar differential equation in the thickness eigendisplacement for the doubly-rotated quartz plates is applied to analyze thickness vibrations of an unelectroded circular plate with free edges at the neighborhood of the pure thickness vibration mode. The scalar differential equation is transformed into an elliptical coordinate system. With the boundary conditions of free edges, the frequencies and the modes are solved in terms of the Mathieu function and the Modified Mathieu function. The results of frequencies of the fundamental harmonic and its third overtone of an AT-cut quartz circular plate by the present approach agree well with the existing theoretical results and the experiment results. The frequencies and modes of an SC-cut quartz circular plate are investigated by the present approach. The frequencies are close to each other when the order of the harmonics is the same. A rotation angle of the symmetric axes of the vibration modes are observed that is dependent on the anisotropic material constants and the order of the harmonics. This approach has potential applications in the design of the doubly-rotated quartz circular resonators.
 https://doi.org/10.1121/1.5050609

[NJK] Pages: 814–821

I. INTRODUCTION

Nowadays, crystal resonators are widely spread in electrical equipment, since they perform well in applications in frequency control, time keeping, sensing, telecommunication, and so on. Among piezoelectric crystals, quartz crystal is the most popular one in the industry due to its high quality and low cost. Usually the key element of the quartz resonators is the quartz plate, mainly operating in the thickness vibration mode (Koga, 1932; Tiersten, 1963). The common shapes of quartz plates are rectangular and circular. The analysis of the finite quartz plate by using the three-dimensional theory of linear elasticity or piezoelectricity is complicated because of anisotropy and the piezoelectric coupling of the quartz crystal.

Much effort has been made to seek for an efficient method for the analysis of the vibrations of crystal plates. Mindlin (1951a) proposed a two-dimensional plate theory considering the effect of rotatory inertia and shear and applied to analyze the vibrations of crystal plates (Mindlin, 1951b; Mindlin and Deresiewicz, 1954). This theory is known as the first-order shear deformation plate theory and is thus suitable for the low-order thickness-shear vibration of crystal plates. Later, a high-order two-dimensional plate theory was proposed (Mindlin, 1961). Following Mindlin's work, extensive analyses of the vibration of the crystal plates have been made, among which the recent work by Wang and Yang (2000), Wang and Zhao (2005), and Zhang *et al.* (2009) should be mentioned. Lee and Nikodem (1972) proposed another two-dimensional plate theory by a series expansion in terms of pure thickness modes for infinite plates, which were in the trigonometric function form. Because of the orthogonality of the trigonometric functions and the simplicity for the derivatives, no increase in complication arose in the approximation of higher order vibration modes. Tiersten and Smythe (1979) constructed a single scalar differential equation with some simplifying assumptions for the analysis of the rotated Y-cut quartz resonators. The numerical calculation was presented for the contoured AT-cut quartz resonators. Similarly, an alternative single scalar differential equation was advised by Stevens and Tiersten (1986) for the doubly-rotated, including the SC-cut (Eernisse, 1975, 1976), quartz resonators.

On the analysis of the thickness-shear vibration modes of the circular quartz crystal plate, Mindlin and Deresiewicz (1954) solved the thickness vibrations of isotropic, elastic plates of a circular shape with free edges by using the first-order shear deformation plate theory, and applied the solution to approximate the frequency spectrum of an AT-cut quartz plate of the circular shape with the help of a proper value of Poisson's ratio $\nu = 0.312$. By using the single scalar differential equation, Tiersten and Smythe (1985) solved the vibration of the AT-cut quartz crystal plates of the rectangular shape. For the circular plate, a perturbation procedure was applied to solve the vibration of the AT-cut quartz plates. For the SC-cut quartz crystal, Stevens and Tiersten (1986) applied the alternative scalar differential equation to analyze the vibrations of plates with rectangular electrodes and contoured plates. Due to the complexity of the theoretical analysis, some researchers used numerical approaches, for example, the works by Yong *et al.* (1992), Wang *et al.* (2009), and Liu *et al.* (2015). Very recently, He *et al.* (2013)

a)Electronic mail: wangji@nbu.edu.cn

improved the analysis of thickness vibrations of the unelectroded AT-cut quartz plates of the circular shape by finding the Mathieu function solutions of the scalar differential equation for the rotated Y-cut quartz plates. Based on the variational form of the scalar differential equation, the Ritz method was used to analyze the vibration of quartz plates in different cases by Shi *et al.* (2014, 2015a,b, 2016a,b). In virtue of the scalar differential equation for the unelectroded and electroded AT-cut quart plates, Zhao *et al.* (2015a,b, 2017) analyzed the vibration of AT-cut quartz rectangular plates with electrode pairs. Wang *et al.* (2017) used the scalar differential equation by Tiersten and Smythe (1985) to analyze the vibrations of partially-electroded quartz circular plates.

In the present analysis, based on the scalar differential equation in the thickness eigendisplacement proposed by Stevens and Tiersten (1986), the vibration frequencies and modes of a doubly-rotated quartz plate at the neighborhood of the pure thickness vibration mode are investigated. The solution of the scalar differential equation for a doubly-rotated quartz plate with free edges is presented in terms of the Mathieu function and the modified Mathieu function. The present method is verified by the comparison with the frequencies of the fundamental thickness vibration mode and the third overtone of an AT-cut quartz circular plate with available experimental and theoretical results. Since the present approach is generally applicable for the doubly-rotated quartz plates, the frequencies and modes in the vicinity of the pure thickness vibration of an SC-cut quartz circular plate are investigated.

II. BASIC EQUATIONS

The conventional components of displacement $\hat{u}_i$ $(i = 1, 2, 3)$ are transformed into a space spanned by the normalized eigenvectors of the piezoelectrically stiffened elastic constant matrix, i.e., Eq. (A8). When it is the pure thickness vibration, only one of three components of the displacement in the transformed space, e.g., u_1, exists. Under the assumption that the so called thickness eigendisplacement, u_1, is dominant, as well as the usual assumptions of small wavenumbers along the plate and small piezoelectric coupling, Stevens and Tiersten (1986) proposed a single scalar differential equation for the vibrations in the vicinity of the pure thickness modes.

Since the thickness-shear modes are of the main interest for quartz resonator, the thickness eigendisplacement is expressed in the odd harmonic form as

$$u_1 = \sum_{n=1,3,5}^{\infty} u_1^{(n)} = \sum_{n=1,3,5}^{\infty} \tilde{u}_1^{(n)}(x_1, x_3, t)\sin(n\pi x_2/2h), \quad (1)$$

where u_1 is the dominant thickness eigendisplacement in the unelectroded quartz plate, $u_1^{(n)}$ is the asymptotic solution function for the u_1 displacement for the nth odd harmonic, and $\tilde{u}_1^{(n)}$ governs the mode shapes along the surface of the unelectroded plate. The homogeneous differential equation proposed by Stevens and Tiersten (1986) is given by

$$M'_n \frac{\partial^2 \tilde{u}_1^{(n)}}{\partial x_1'^2} + P'_n \frac{\partial^2 \tilde{u}_1^{(n)}}{\partial x_3'^2} - \frac{n^2\pi^2 \bar{c}^{(1)}}{4h^2}\tilde{u}_1^{(n)} - \rho\ddot{\tilde{u}}_1(n) = 0, \quad (2)$$

where the coordinates x_i' are rotated from the conventional coordinates x_i, and the detailed expressions for the variables and parameters are listed in the Appendix.

When $M'_n > P'_n$, we set

$$x_1' = \lambda c \sinh\xi \sin\eta, \quad x_3' = \mu c \cosh\xi \cos\eta, \quad (3)$$

where

$$\lambda = \frac{1}{\omega_0}\sqrt{\frac{M'_n}{\rho}}, \quad \mu = \frac{1}{\omega_0}\sqrt{\frac{P'_n}{\rho}}. \quad (4)$$

When $M'_n < P'_n$, we set

$$x_3' = \lambda c \sinh\xi \sin\eta, \quad x_1' = \mu c \cosh\xi \cos\eta, \quad (5)$$

where

$$\lambda = \frac{1}{\omega_0}\sqrt{\frac{P'_n}{\rho}}, \quad \mu = \frac{1}{\omega_0}\sqrt{\frac{M'_n}{\rho}}. \quad (6)$$

In both cases, we have

$$\omega_0 = \frac{n\pi}{2h}\sqrt{\frac{\bar{c}^{(1)}}{\rho}}, \quad c = \sqrt{\frac{R^2}{\mu^2} - \frac{R^2}{\lambda^2}}. \quad (7)$$

Under the above transformation and the ignoring of the harmonic time factor, the differential equation, i.e., Eq. (2), for a circular plate in the thickness eigendisplacement $\tilde{u}_1^{(n)}$ becomes a differential equation in the elliptical coordinate system (ξ, η) taking the following form:

$$\frac{\partial^2 \tilde{u}_1^{(n)}}{\partial \xi^2} + \frac{\partial^2 \tilde{u}_1^{(n)}}{\partial \eta^2} + 2q[\cosh 2\xi - \cos 2\eta]\tilde{u}_1^{(n)} = 0, \quad (8)$$

where

$$q = \frac{c^2}{4}\left(\frac{\omega^2}{\omega_0^2} - 1\right). \quad (9)$$

The circular boundary in the Cartesian coordinates (x_1, x_3) or (x_1', x_3'), i.e., $x_1^2 + x_3^2 = x_1'^2 + x_3'^2 = R^2$, becomes the boundary in the elliptical coordinates given by $\xi = \xi_0$, where R is the radius of the circular, and ξ_0 satisfies

$$\tanh\xi_0 = \frac{\mu}{\lambda}. \quad (10)$$

Furthermore, in virtue of the standard method of the separation of variables, i.e.,

$$\tilde{u}_1^{(n)}(\xi, \eta) = U(\xi)V(\eta). \quad (11)$$

Equation (8) yields

$$\frac{d^2V(\eta)}{d\eta^2} + (a - 2q\cos 2\eta)V(\eta) = 0, \quad (12)$$

$$\frac{d^2U(\xi)}{d\xi^2} + (2q\cosh 2\xi - a)U(\xi) = 0. \tag{13}$$

The differential equation, Eq. (8), yields two related one-dimensional differential equations; Eq. (12) is the Mathieu equation, and Eq. (13) is the modified Mathieu equation.

Given q, the Mathieu equation, Eq. (12), has infinitely many solutions with period π or period 2π. The solutions are the Mathieu cosine $\mathrm{ce}_m(\eta, q)$ and the Mathieu sine $\mathrm{se}_m(\eta, q)$. Every solution is determined by a specific value of a, referred to as a characteristic value, which might be denoted as a_m for the Mathieu cosine $\mathrm{ce}_m(\eta, q)$, and b_m for the Mathieu sine $\mathrm{se}_m(\eta, q)$. For fixed q and a_m or b_m, the modified Mathieu equation has solutions denoted by $\mathrm{Ce}_m(\xi, q)$ or $\mathrm{Se}_m(\xi, q)$, which satisfy (McLachlan, 1947)

$$\mathrm{Ce}_m(\xi,q) = \mathrm{ce}_m(i\xi,q), \quad \mathrm{Se}_m(\xi,q) = -i\mathrm{se}_m(i\xi,q), \quad i = \sqrt{-1}. \tag{14}$$

The vibration modes at a specific frequency might be characterized by

$$\mathrm{Ce}_m(\xi,q)\mathrm{ce}_m(\eta,q), \quad \mathrm{Se}_m(\xi,q)\mathrm{se}_m(\eta,q). \tag{15}$$

Therefore, the general solution $\tilde{u}_1^{(n)}$ of the differential Eq. (8) is obtained as

$$\tilde{u}_1^{(n)} = \sum_{m=0}^{\infty} C_m \mathrm{Ce}_m(\xi,q)\mathrm{ce}_m(\eta,q) + \sum_{m=1}^{\infty} S_m \mathrm{Se}_m(\xi,q)\mathrm{se}_m(\eta,q), \tag{16}$$

where C_m and S_m are undetermined constants.

As in previous works (Tiersten and Smythe, 1985; He *et al.*, 2013), the boundary condition is given by

$$\tilde{u}_1^{(n)} = 0. \tag{17}$$

Since the boundary is at $\xi = \xi_0$, we have

$$\sum_{m=0}^{\infty} C_m \mathrm{Ce}_m(\xi_0,q)\mathrm{ce}_m(\eta,q) + \sum_{m=1}^{\infty} S_m \mathrm{Se}_m(\xi_0,q)\mathrm{se}_m(\eta,q) = 0. \tag{18}$$

With the orthogonal relations of the Mathieu cosine $\mathrm{ce}_m(\eta, q)$ and the Mathieu sine $\mathrm{se}_m(\eta, q)$ (Arfken *et al.*, 2012), i.e.

$$\int_0^{2\pi} \mathrm{ce}_m \mathrm{ce}_n d\eta = \int_0^{2\pi} \mathrm{se}_m \mathrm{se}_n d\eta = 0, \quad m \neq n; \qquad \int_0^{2\pi} \mathrm{ce}_m \mathrm{se}_n d\eta = 0, \tag{19}$$

the multiplication of Eq. (18) with the Mathieu cosine $\mathrm{ce}_i(\eta, q)$ or the Mathieu sine $\mathrm{se}_i(\eta, q)$ followed by the integration in η from 0 to 2π leads to the equations for the determination of the values of q on the boundary, i.e.,

$$\mathrm{Ce}_m(\xi_0,q) = 0, m = 0,1,\ldots, \quad \text{or } \mathrm{Se}_m(\xi_0,q) = 0, \quad m = 1,2,\ldots. \tag{20}$$

Every equation in Eq. (20) has many roots, which leads to infinitely many values of q. Every value of q determines a frequency, according to Eq. (9), whose alternative form is the frequency equation given by

$$\frac{\omega}{\omega^*} = \sqrt{\alpha_n \frac{h^2}{R^2} + n^2}, \tag{21}$$

where

$$\alpha_n = \frac{16qM_n'P_n'}{\pi^2 \bar{c}^{(1)} |P_n' - M_n'|}, \tag{22}$$

and ω^* is the value of ω_0 when $n = 1$.

III. NUMERICAL EXAMPLES

The formulae in the above section are generally applicable for the doubly-rotated case. They are implemented in the software MATHEMATICA, which has the built-in Mathieu functions. In the following calculations, the thickness eigendisplacement u_1 is properly chosen to represent the C mode in the pure thickness vibration, since the main interest is of the vibrations at the neighborhood of the C mode. If the interest is of the vibrations at the neighborhood of the B mode, the thickness eigendisplacement u_1 should be chosen to represent the B mode in the pure thickness vibration.

The correctness of these formulae is confirmed by the numerical results of the fundamental frequency when $n = 1$ and its third overtone when $n = 3$ of a AT-cut quartz circular plate. The results of the present method are 15.0798 MHz and 45.2103 MHz, respectively, which are of high accuracy compared with the values given by the experiments and theoretical predictions (Tiersten and Smythe, 1985; He *et al.*, 2013). The material constants of the AT-cut quartz crystal are obtained by rotating the intrinsic coordinates of the quartz crystal about the x axis by angle $\theta = 35.25°$. The material constants of the quartz crystal in the intrinsic coordinate system were given by Bechmann (1958). Following the configuration given by Tiersten and Smythe (1985), the circular plate has a diameter of $2R = 7.874$ mm and a thickness of $2h = 0.110236$ mm.

The slight difference between the values of frequencies calculated by the present method and by He *et al.* (2013) mainly comes from the truncation errors of the material constants. When the specific material constants for the AT-cut quart crystal (Tiersten, 1969) are used in the present method, the frequencies of the fundamental mode and its third overtone of an AT-cut quartz circular plate are 15.079091 MHz and 45.208327 MHz, respectively. The remaining difference might come from the difference in the parameter M_n and P_n for different cases. When the scalar differential equation for the doubly-rotated quartz plates (Stevens and Tiersten, 1986) is specific for the AT-cut quartz plate, the values of parameters Q_n are consistent with the values in the scalar differential equation for the AT-cut quartz plates (Tiersten and Smythe, 1985), i.e., $Q_n = 0$, but the values of the parameters

TABLE I. The frequencies of the SC-cut quartz circular plate with a diameter of $2R = 7.874$ mm and a thickness of $2h = 0.110236$ mm ($R/h = 71.429$) at the neighborhood of the frequencies of the pure thickness vibration mode.

	Ce_m (MHz)				Se_m (MHz)			
	0	1	2	3	1	2	3	4
$n = 1$	16.3173	16.3274	16.3420	16.3610	16.3330	16.3471	16.3651	16.3869
	16.3583	16.3776	16.4013	16.4299	16.3925	16.4166	16.4448	16.4772
	16.4358	16.4647	16.4977	16.5349	16.4879	16.5216	16.5594	16.6012
$n = 3$	48.9288	48.9318	48.9361	48.9415	48.9323	48.9364	48.9415	48.9477
	48.9381	48.9442	48.9519	48.9610	48.9457	48.9530	48.9616	48.9714
	48.9554	48.9643	48.9749	48.9872	48.9671	48.9773	48.9890	49.0021

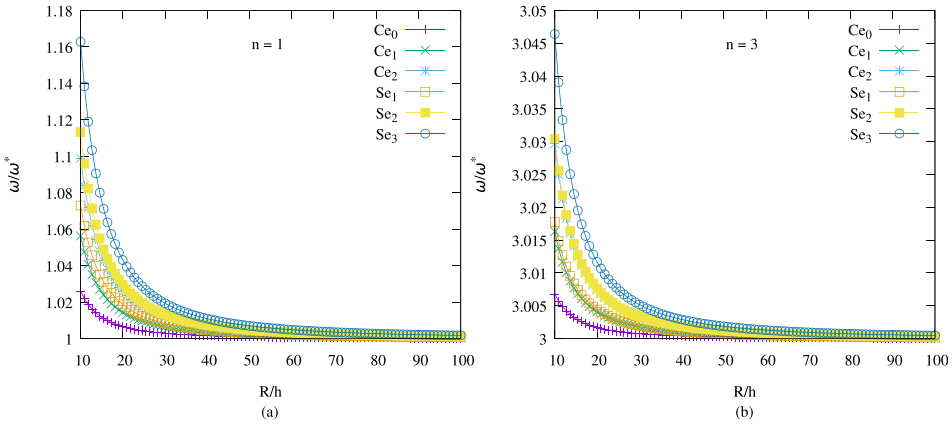

FIG. 1. (Color online) Frequency spectrum of an SC-cut quartz circular plate by finding the first roots of $Ce_m = 0$ and $Se_m = 0$ when $n = 1, 3$.

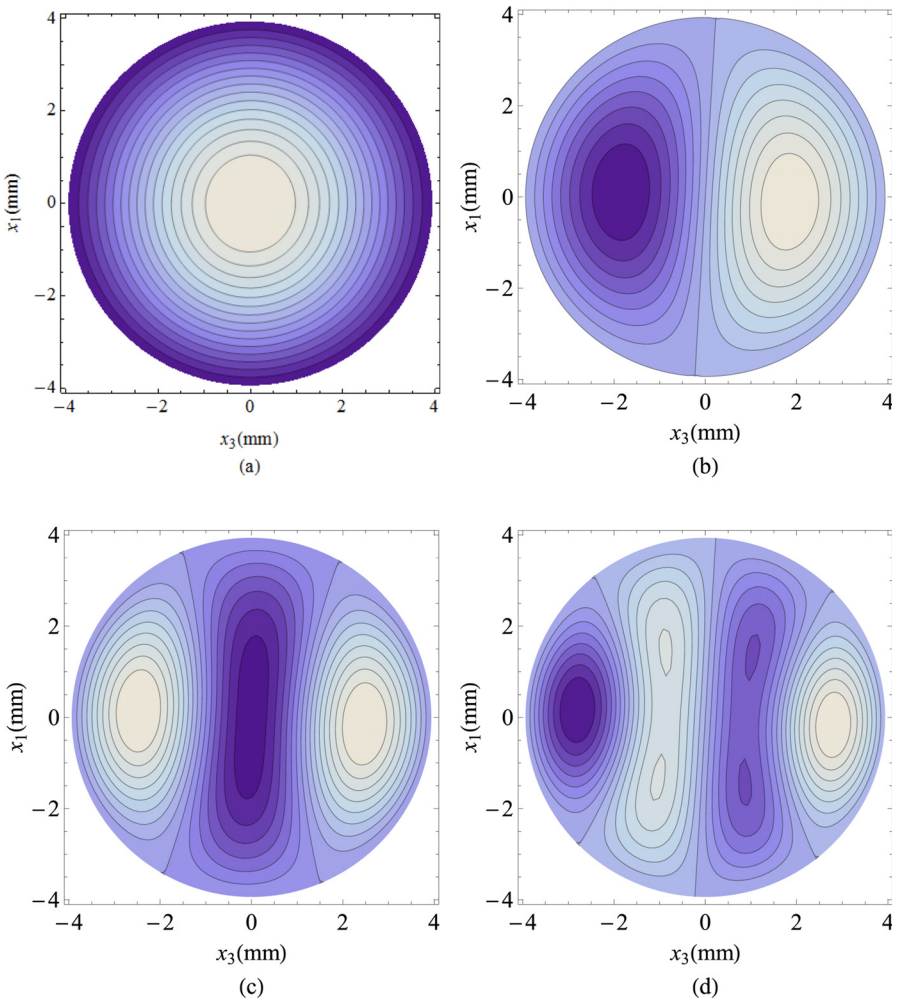

FIG. 2. (Color online) The modes of Ce_mce_m at the first frequencies given by $Ce_m = 0$ when $n = 1$ for different values of m: (a) $m = 0$, (b) $m = 1$, (c) $m = 2$, (d) $m = 3$.

M_n and P_n are slightly different. The expressions of M_n, Q_n, and P_n for the doubly-rotated quartz plates are given by Eq. (A2).

In the following numerical examples, the SC-cut quartz circular plate is chosen. The material constants of the SC-cut quartz crystal are obtained by rotating the intrinsic coordinates of the quartz crystal about the z axis by angle $\phi = 21.93°$ and then about the new x axis by angle $\theta = 33.93°$.

A. Frequencies of the vibrations

Once the boundary value of ξ_0 is determined by Eq. (10), more than one value of q for the fixed value of m is obtained as a solution of Eq. (20), and then more than one frequency $\omega/2\pi$ is calculated by Eq. (9). The frequencies of vibrations of the SC-cut quartz circular plate, corresponding to the first three roots of Eq. (20), are listed in Table I. The values of the frequencies at the nth row are related with the nth roots of Eq. (20). They are very close to each other when n is the same, and are around the value of $\omega_0/2\pi$ calculated by Eq. (7), which is 16.3439 MHz when $n = 1$ and 49.0316 MHz when $n = 3$. According to Eq. (21), the frequency becomes infinite when the ratio of diameter to thickness R/h approaches zero, and becomes a constant when the ratio approaches infinite. The relation between the normalized frequency corresponding to the first root of Eq. (20) and the ratio of diameter to thickness is shown in Fig. 1 for different n and m.

B. Vibration modes

In the present analysis, the vibration of the quartz circular plate in the vicinity of the odd pure thickness frequency is described by the thickness eigendisplacement u_1, and the vibration modes might be represented by $\mathrm{Ce}_m\mathrm{ce}_m$ and $\mathrm{Se}_m\mathrm{se}_m$ in Eq. (15) with the corresponding frequencies calculated by the boundary condition in Eq. (20).

Figures 2–5 are contours of the modes of $\mathrm{Ce}_m\mathrm{ce}_m$ and $\mathrm{Se}_m\mathrm{se}_m$ when $n = 1$. The value is larger at lighter shading and lower at darker shading. A small angle between the symmetry axes of the vibrations and the coordinates is observed, which is equal to the value of $\hat{\beta}_n$ defined by Eq. (A5). The value of $\hat{\beta}_n$ when $n = 1$ is $-1.66°$. The angle is related to the anisotropy property of quartz crystal and the value of n. The symmetry axes might be denoted as x_1' and x_3', respectively. Figure 2 shows the $\mathrm{Ce}_m\mathrm{ce}_m$ modes of the vibrations of the quartz circular plate when $n = 1$. The $\mathrm{Ce}_m\mathrm{ce}_m$ mode is symmetric about both the x_3' and x_1' axes when $n = 1$, $m = 0$, 2, but symmetric about the x_3' axis and antisymmetric about the x_1' axis when $n = 1$, $m = 1$, 3. Figure 3 shows that the $\mathrm{Se}_m\mathrm{se}_m$ modes when $n = 1$ are antisymmetric about the axis x_3' and symmetric about the axis x_1' when $m = 1$, 3, but antisymmetric about both the x_3' and x_1' axes when $m = 2$, 4. By using the

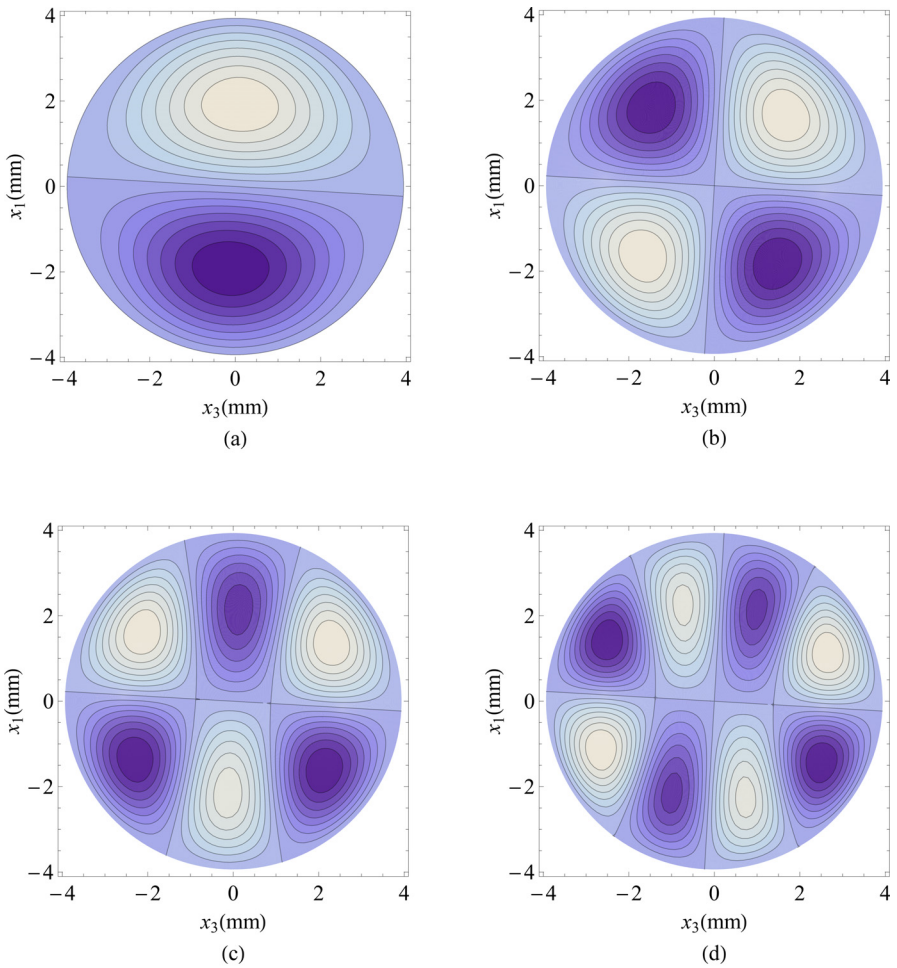

FIG. 3. (Color online) The modes of $\mathrm{Se}_m\mathrm{se}_m$ at the first frequencies given by $\mathrm{Se}_m = 0$ when $n = 1$ for different values of m: (a) $m = 1$, (b) $m = 2$, (c) $m = 3$, (d) $m = 4$.

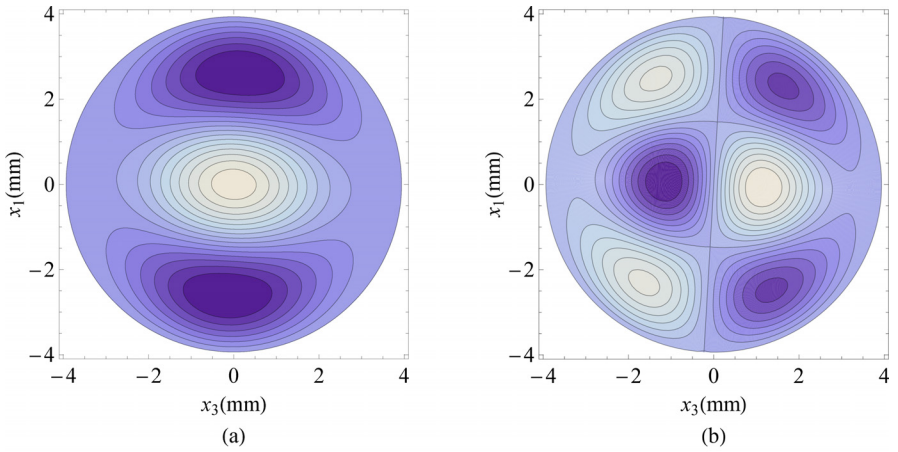

FIG. 4. (Color online) The modes of $\mathrm{Ce}_m\mathrm{ce}_m$ at the second frequencies given by $\mathrm{Ce}_m = 0$ when $n = 1$ for different values of m: (a) $m = 0$, (b) $m = 1$, (c) $m = 2$, (d) $m = 3$.

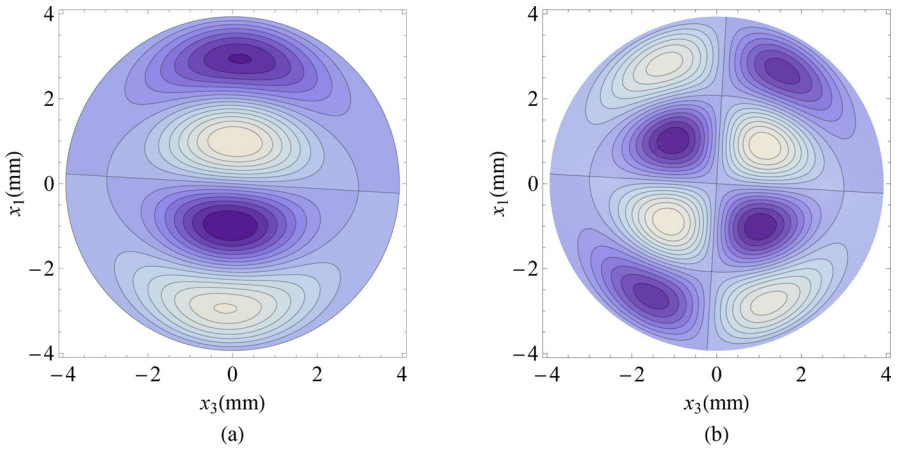

FIG. 5. (Color online) The modes of $\mathrm{Se}_m\mathrm{se}_m$ at the second frequencies given by $\mathrm{Se}_m = 0$ when $n = 1$ for different values of m: (a) $m = 1$, (b) $m = 2$, (c) $m = 3$, (d) $m = 4$.

present method, the Ce_mce_m and Se_mse_m modes of vibration of the quartz circular plate when $n=3$ are quite similar with those when $n=1$, but the rotation angle $\hat{\beta}_n$, which is dependent on the material constants and the value of n, is much larger. Figures 4 and 5 are the vibration modes of the quartz circular plate at the second frequencies when $n=1$, which are modes of higher order.

IV. CONCLUSIONS

The scalar differential equation in the thickness eigendisplacement proposed by Stevens and Tiersten (1986) is used to analyze the vibration of a circular plate of the doubly-rotated quartz crystal with free edges in the vicinity of the thickness vibration mode. The correctness of the formulation is confirmed by the numerical results of the frequencies of the fundamental mode and its third overtone of an AT-cut quartz circular plate. The frequencies and modes of an SC-cut quartz circular plate at the neighborhood of the pure thickness vibration mode are presented. The results are helpful in the design of SC-cut quartz crystal resonators. The newly proposed approach is applicable for the analysis of the vibration of a doubly-rotated quartz circular plate in general.

ACKNOWLEDGMENTS

The first author would like to thank Professor Jiashi Yang from the University of Nebraska-Lincoln for his professional and friendly suggestion on the use of the scalar differential equation for the analysis of a circular crystal plate during his stay at Ningbo University in December 2017. This research is supported by the China Postdoctoral Science Foundation (No. 2017M621893), the National Natural Science Foundation of China (Nos. 11372145 and 11672142), and the K.C. Wong Magna Fund in Ningbo University.

APPENDIX: VARIABLES AND PARAMETERS FOR THE SCALAR DIFFERENTIAL EQUATION

The parameters needed in the numerical calculation are listed here for a self-documented reason; for more details, readers are referred to the work by Stevens and Tiersten (1986).

The variables M_n' and P_n' in Eq. (2) are given by

$$M_n' = M_n\cos^2\hat{\beta}_n - Q_n\sin\hat{\beta}_n\cos\hat{\beta}_n + P_n\sin^2\hat{\beta}_n,$$
$$P_n' = M_n\sin^2\hat{\beta}_n + Q_n\sin\hat{\beta}_n\cos\hat{\beta}_n + P_n\cos^2\hat{\beta}_n, \quad \text{(A1)}$$

where

$$M_n = c_{11} - \frac{c_{16}^2}{\bar{c}^{(1)}} + r_2(c_{12}+c_{66}) + r_5(c_{17}+c_{86}) + \frac{4\left(r_2\bar{c}^{(1)} - c_{66}\right)\left(r_2\bar{c}^{(2)} + c_{12}\right)}{\bar{c}^{(2)}\kappa_2 n\pi}\cot\kappa_2\frac{n\pi}{2} + \frac{4\left(r_5\bar{c}^{(1)} - c_{86}\right)\left(r_5\bar{c}^{(3)} + c_{17}\right)}{\bar{c}^{(3)}\kappa_3 n\pi}\cot\kappa_3\frac{n\pi}{2},$$

$$Q_n = 2c_{51} - \frac{2c_{16}c_{56}}{\bar{c}^{(1)}} + r_2(c_{52}+c_{76}) + r_4(c_{12}+c_{66}) + r_3(c_{17}+c_{86}) + r_5(c_{36}+c_{57}) + 4\frac{\left(r_2\bar{c}^{(1)} - c_{66}\right)\left(r_4\bar{c}^{(2)} + c_{52}\right) + \left(r_2\bar{c}^{(2)} + c_{12}\right)\left(r_4\bar{c}^{(1)} - c_{76}\right)}{\bar{c}^{(2)}\kappa_2 n\pi}\cot\kappa_2\frac{n\pi}{2} + 4\frac{\left(r_5\bar{c}^{(1)} - c_{86}\right)\left(r_3\bar{c}^{(3)} + c_{57}\right) + \left(r_5\bar{c}^{(3)} + c_{17}\right)\left(r_3\bar{c}^{(1)} - c_{36}\right)}{\bar{c}^{(3)}\kappa_3 n\pi}\cot\kappa_3\frac{n\pi}{2},$$

$$P_n = c_{58} - \frac{c_{56}^2}{\bar{c}^{(1)}} + r_4(c_{52}+c_{76}) + r_3(c_{36}+c_{57}) + \frac{4\left(r_4\bar{c}^{(1)} - c_{76}\right)\left(r_4\bar{c}^{(2)} + c_{52}\right)}{\bar{c}^{(2)}\kappa_2 n\pi}\cot\kappa_2\frac{n\pi}{2} + \frac{4\left(r_3\bar{c}^{(1)} - c_{36}\right)\left(r_3\bar{c}^{(3)} + c_{57}\right)}{\bar{c}^{(3)}\kappa_3 n\pi}\cot\kappa_3\frac{n\pi}{2}, \quad \text{(A2)}$$

in which

$$r_2 = \frac{c_{12}+c_{66}}{\bar{c}^{(1)} - \bar{c}^{(2)}}, \quad r_3 = \frac{c_{36}+c_{57}}{\bar{c}^{(1)} - \bar{c}^{(3)}},$$
$$r_4 = \frac{c_{52}+c_{76}}{\bar{c}^{(1)} - \bar{c}^{(2)}}, \quad r_5 = \frac{c_{17}+c_{86}}{\bar{c}^{(1)} - \bar{c}^{(3)}}, \quad \text{(A3)}$$

$$\kappa_2 = \sqrt{\bar{c}^{(1)}/\bar{c}^{(2)}}, \quad \kappa_3 = \sqrt{\bar{c}^{(1)}/\bar{c}^{(3)}}. \quad \text{(A4)}$$

The new Cartesian coordinates are related to the conventional Cartesian coordinates by the transformation $x_i' = R_{ij}x_j$, where

$$R_{ij} = \begin{bmatrix} \cos\hat{\beta}_n & 0 & -\sin\hat{\beta}_n \\ 0 & 1 & 0 \\ \sin\hat{\beta}_n & 0 & \cos\hat{\beta}_n \end{bmatrix},$$
$$\hat{\beta}_n = \frac{1}{2}\tan^{-1}\left(\frac{-Q_n}{M_n - P_n}\right), \quad \text{(A5)}$$

$\bar{c}^{(i)}$ $(i=1,2,3)$ are the three real, positive roots of the cubic equation

$$|\bar{\bar{c}}_{2nr2} - \bar{c}\delta_{nr}| = 0, \quad \text{(A6)}$$

where

$$\overline{\hat{c}}_{2nr2} = \hat{c}_{2nr2} + \hat{e}_{22n}\hat{e}_{22r}/\epsilon_{22}, \tag{A7}$$

or in the matrix form

$$\begin{bmatrix} \hat{c}_{66}+\hat{e}_{26}\hat{e}_{26}/\epsilon_{22} & \hat{c}_{26}+\hat{e}_{22}\hat{e}_{26}/\epsilon_{22} & \hat{c}_{46}+\hat{e}_{24}\hat{e}_{26}/\epsilon_{22} \\ \hat{c}_{26}+\hat{e}_{22}\hat{e}_{26}/\epsilon_{22} & \hat{c}_{22}+\hat{e}_{22}\hat{e}_{22}/\epsilon_{22} & \hat{c}_{24}+\hat{e}_{22}\hat{e}_{24}/\epsilon_{22} \\ \hat{c}_{46}+\hat{e}_{24}\hat{e}_{26}/\epsilon_{22} & \hat{c}_{24}+\hat{e}_{22}\hat{e}_{24}/\epsilon_{22} & \hat{c}_{44}+\hat{e}_{24}\hat{e}_{24}/\epsilon_{22} \end{bmatrix}. \tag{A8}$$

Note in our numerical calculation, $\bar{c}^{(1)}$ is of the minimum value and $\hat{c}_{ijkl}$, $\hat{e}_{mkl}$, and ϵ_{ij} are the elasticity tensor, piezoelectricity tensor, and the dielectric tensor of the SC-cut quartz crystal, respectively.

The parameters c_{ij} in Eq. (A2) are the contracted form of the fourth order tensor c_{ijkl} with the mapping used by Stevens and Tiersten (1986).

Arfken, G., Weber, H., and Harris, F. (**2012**). *Mathematical Methods for Physicists: A Comprehensive Guide* (Academic Press, New York), pp. 1–29.

Bechmann, R. (**1958**). "Elastic and piezoelectric constants of alpha-quartz," Phys. Rev. **110**(5), 1060–1061.

Eernisse, E. P. (**1975**). "Quartz resonator frequency shifts arising from electrode stress," in *Proceedings of the 29th Annual Symposium on Frequency Control*, May 28–30, Fort Monmouth, NJ, pp. 1–4.

Eernisse, E. P. (**1976**). "Calculations on the stress compensated (sc-cut) quartz resonator," in *Proceedings* 30th Annual Symposium on Frequency Control, June 2–4, Fort Monmouth, NJ, pp. 8–11.

He, H., Yang, J., and Jiang, Q. (**2013**). "Thickness-shear and thickness-twist vibrations of circular AT-cut quartz resonators," Acta Mech. Solid. Sin. **26**(3), 245–254.

Koga, I. (**1932**). "Thickness vibrations of piezoelectric oscillating crystals," J. Appl. Phys. **3**(2), 70–80.

Lee, P., and Nikodem, Z. (**1972**). "An approximate theory for high-frequency vibrations of elastic plates," Int. J. Solids Struct. **8**(5), 581–612.

Liu, B., Xing, Y., Wang, W., and Yu, W. (**2015**). "Thickness-shear vibration analysis of circular quartz crystal plates by a differential quadrature hierarchical finite element method," Compos. Struct. **131**, 1073–1080.

McLachlan, N. W. (**1947**). *Theory and Application of Mathieu Functions* (Clarendon Press, London), p. 401.

Mindlin, R. D. (**1951a**). "Influence of rotatory inertia and shear on flexural motions of isotropic, elastic plates," J. Appl. Mech. Trans. ASME **18**, 31–38.

Mindlin, R. D. (**1951b**). "Thickness-shear and flexural vibrations of crystal plates," J. Appl. Phys. **22**(3), 316–323.

Mindlin, R. D. (**1961**). "High frequency vibrations of crystal plates," Q. Appl. Math. **19**(1), 51–61.

Mindlin, R. D., and Deresiewicz, H. (**1954**). "Thickness-shear and flexural vibrations of a circular disk," J. Appl. Phys. **25**(10), 1329–1332.

Shi, J., Fan, C., Zhao, M., and Yang, J. (**2014**). "Variational formulation of the Stevens-Tiersten equation and application in the analysis of rectangular trapped-energy quartz resonators," J. Acoust. Soc. Am. **135**(1), 175–181.

Shi, J., Fan, C., Zhao, M., and Yang, J. (**2015a**). "Trapped thickness-shear modes in a contoured, partially electroded AT-cut quartz resonator," Eur. Phys. J. Appl. Phys. **69**(1), 10302.

Shi, J., Fan, C., Zhao, M., and Yang, J. (**2015b**). "Variational analysis of thickness-shear vibrations of a quartz piezoelectric plate with two pairs of electrodes as an acoustic wave filter," Int. J. Appl. Electromagn. Mech. **47**(4), 951–961.

Shi, J., Fan, C., Zhao, M., and Yang, J. (**2016a**). "Energy trapping of thickness-shear modes in inverted-mesa AT-cut quartz piezoelectric resonators," Ferroelectrics **494**(1), 157–169.

Shi, J., Fan, C., Zhao, M., and Yang, J. (**2016b**). "Thickness-shear vibration characteristics of an AT-cut quartz resonator with rectangular ring electrodes," Int. J. Appl. Electromagn. Mech. **51**(1), 1–10.

Stevens, D. S., and Tiersten, H. F. (**1986**). "An analysis of doubly rotated quartz resonators utilizing essentially thickness modes with transverse variation," J. Acoust. Soc. Am. **79**(6), 1811–1826.

Tiersten, H. F. (**1963**). "Thickness vibrations of piezoelectric plates," J. Acoust. Soc. Am. **35**(1), 53–58.

Tiersten, H. F. (**1969**). *Linear Piezoelectric Plate Vibrations* (Springer, Boston, MA).

Tiersten, H. F., and Smythe, R. C. (**1979**). "An analysis of contoured crystal resonators operating in overtones of coupled thickness shear and thickness twist," J. Acoust. Soc. Am. **65**(6), 1455–1460.

Tiersten, H. F., and Smythe, R. C. (**1985**). "Coupled thickness-shear and thickness-twist vibrations of unelectroded AT-cut quartz plates," J. Acoust. Soc. Am. **78**(5), 1684–1689.

Wang, B., Dai, X., Zhao, X., and Qian, Z. (**2017**). "A semi-analytical solution for the thickness-vibration of centrally partially-electroded circular AT-cut quartz resonators," Sensors **17**(8), 1820.

Wang, J., Shi, J., and Du, J.-K. (**2009**). "The finite element analysis of thickness-shear vibrations of quartz crystal plates with ANSYS," in *Proceedings of the 2009 Symposium on Piezoelectricity, Acoustic Waves, and Device Applications (SPAWDA 2009)*, December 17–20, Wuhan, China, pp. 124–124.

Wang, J., and Yang, J. (**2000**). "Higher-order theories of piezoelectric plates and applications," Appl. Mech. Rev. **53**(4), 87–89.

Wang, J., and Zhao, W. (**2005**). "The determination of the optimal length of crystal blanks in quartz crystal resonators," IEEE Trans. Ultrason. Ferroelectr. Freq. Control **52**(11), 2023–2030.

Yong, Y.-K., Stewart, J., Detaint, J., Zarka, A., Capelle, B., and Zheng, Y. (**1992**). "Thickness-shear mode shapes and mass-frequency influence surface of a circular and electroded AT-cut quartz resonator," IEEE Trans. Ultrason. Ferroelectr. Freq. Control **39**(5), 609–617.

Zhang, C. L., Chen, W. Q., and Yang, J. S. (**2009**). "Electrically forced vibration of a rectangular piezoelectric plate of monoclinic crystals," Int. J. Appl. Electromagn. Mech. **31**(4), 207–218.

Zhao, Z., Qian, Z., and Wang, B. (**2017**). "Thickness-shear vibration of a Z-strip AT-cut quartz crystal plate with nonuniform electrode pairs," Ferroelectrics **506**(1), 48–62.

Zhao, Z., Qian, Z., Wang, B., and Yang, J. (**2015a**). "Analysis of thickness-shear and thickness-twist modes of AT-cut quartz acoustic wave resonator and filter," Appl. Math. Mech. **36**(12), 1527–1538.

Zhao, Z., Qian, Z., Wang, B., and Yang, J. (**2015b**). "Thickness-shear and thickness-twist modes in an AT-cut quartz acoustic wave filter," Ultrasonics **58**, 1–5.